

Fractional Quantum Hall Effect at $\nu = 1/2$ in Hole Systems Confined to GaAs Quantum Wells

Yang Liu, A.L. Graninger, S. Hasdemir, M. Shayegan, L.N. Pfeiffer, K.W. West, and K.W. Baldwin
Department of Electrical Engineering, Princeton University, Princeton, New Jersey 08544

R. Winkler
*Department of Physics, Northern Illinois University, DeKalb, Illinois 60115 and
 Materials Science Division, Argonne National Laboratory, Argonne, Illinois 60439, USA*
 (Dated: June 10, 2021)

We observe fractional quantum Hall effect (FQHE) at the even-denominator Landau level filling factor $\nu = 1/2$ in two-dimensional hole systems confined to GaAs quantum wells of width 30 to 50 nm and having bilayer-like charge distributions. The $\nu = 1/2$ FQHE is stable when the charge distribution is symmetric and only in a range of intermediate densities, qualitatively similar to what is seen in two-dimensional electron systems confined to approximately twice wider GaAs quantum wells. Despite the complexity of the hole Landau level structure, originating from the coexistence and mixing of the heavy- and light-hole states, we find the hole $\nu = 1/2$ FQHE to be consistent with a two-component, Halperin-Laughlin (Ψ_{331}) state.

In a large perpendicular magnetic field (B), interacting two-dimensional electron systems (2DESs) exhibit fractional quantum Hall effect (FQHE) [1], predominantly at odd-denominator Landau level (LL) filling factors ν [2]. Much more rarely, FQHE is observed at *even-denominator* fillings such as $\nu = 5/2$ [3] and $1/2$ [4, 5]. The origin of these states has long been enigmatic. The $5/2$ FQHE is likely to be the one-component, Moore-Read (Pfaffian) state [6], a state that is expected to obey non-Abelian statistics and find use in topological quantum computing [7]. Alternatively, it might be a two-component, Abelian, Halperin-Laughlin (Ψ_{331}) state [8], if the spin degree of freedom is necessary. The $\nu = 1/2$ FQHE has been reported in 2DESs confined either to double quantum wells (QWs) [5], or to symmetric, wide, single QWs where the electrons typically occupy two electric subbands and have a bilayer-like charge distribution [4]. It is generally believed to be a Ψ_{331} state, with the two pseudo-spin components being the symmetric and antisymmetric electric subbands or, equivalently, the two "layers" which can be constructed from a linear combination of the subbands. The Ψ_{331} state is stable when the Coulomb energy is much larger than the pseudo-spin splitting (the subband energy separation), and the inter-layer and intra-layer Coulomb energies are comparable [4, 5, 9–17]. While these conditions are clearly met for the $\nu = 1/2$ FQHE observed in double QWs, the case for the wide QWs is less clear: The subband separation in wide QWs is large and in principle a one-component, Pfaffian state at $\nu = 1/2$ can be stabilized [18].

Up to now, the $\nu = 1/2$ FQHE has only been observed in GaAs 2DESs and, very recently, in bilayer graphene [19]. Here we report the first observation of FQHE at $\nu = 1/2$ in very high-quality 2D *hole* systems (2DHSs) confined to relatively wide GaAs QWs. Thanks to the coexistence of heavy-hole (HH) and light-hole (LH) states, as well as the strong spin-orbit interaction and HH-LH

mixing, the LL structure of 2DHSs confined to wide QWs is quite complex and non-linear and it includes multiple level crossings and anti-crossings [20]. Despite these complexities, far from the LL crossings, the hole $\nu = 1/2$ FQHE exhibits qualitatively the same evolution as in 2DESs. It is only stable in symmetric QWs, emerges from a compressible state at low densities, and is destroyed by an insulating phase at high densities. Based on a detailed discussion of the data, we conclude that, although we cannot rule out the possibility that the strong LL mixing may stabilize a single-component $1/2$ state, the $\nu = 1/2$ FQHE in our 2DHSs is consistent with a two-component Ψ_{331} state.

Our samples are made from GaAs wafers grown by molecular beam epitaxy along the (001) direction. The 2DHSs are confined to GaAs QWs with widths $W = 30$ to 50 nm, flanked by undoped $\text{Al}_{0.3}\text{Ga}_{0.7}\text{As}$ spacer layers and carbon δ -doped layers, and have a very high mobility $\mu \gtrsim 200 \text{ m}^2/\text{Vs}$ at low temperatures. We made $4 \times 4 \text{ mm}^2$ samples in a van der Pauw geometry with alloyed In:Zn contacts at their four corners. We then fitted each sample with an evaporated Ti/Au front-gate and an In back-gate to control the charge distribution symmetry in the QW and 2D hole density, p , which we give throughout this letter in units of 10^{11} cm^{-2} . All the measurements were carried out in dilution refrigerators at their base temperature ($T \simeq 30 \text{ mK}$).

Figure 1 highlights our main finding: the observation of $\nu = 1/2$ FQHE in 2DHSs confined to GaAs QWs. Data are shown for QWs with different W and p . The $\nu = 1/2$ FQHE is evidenced by a very deep minimum in the longitudinal resistance (R_{xx}) at $\nu = 1/2$, accompanied by a Hall resistance (R_{xy}) plateau, well-quantized at $2h/e^2$.

Figure 2 shows a waterfall plot of R_{xx} and R_{xy} vs $1/\nu$ traces for $p = 1.03$ to 1.74 taken in the 40-nm-wide QW. At the lowest p the 2DHS is compressible at $\nu = 1/2$ and FQH states are seen only at odd-denominator fillings $\nu =$

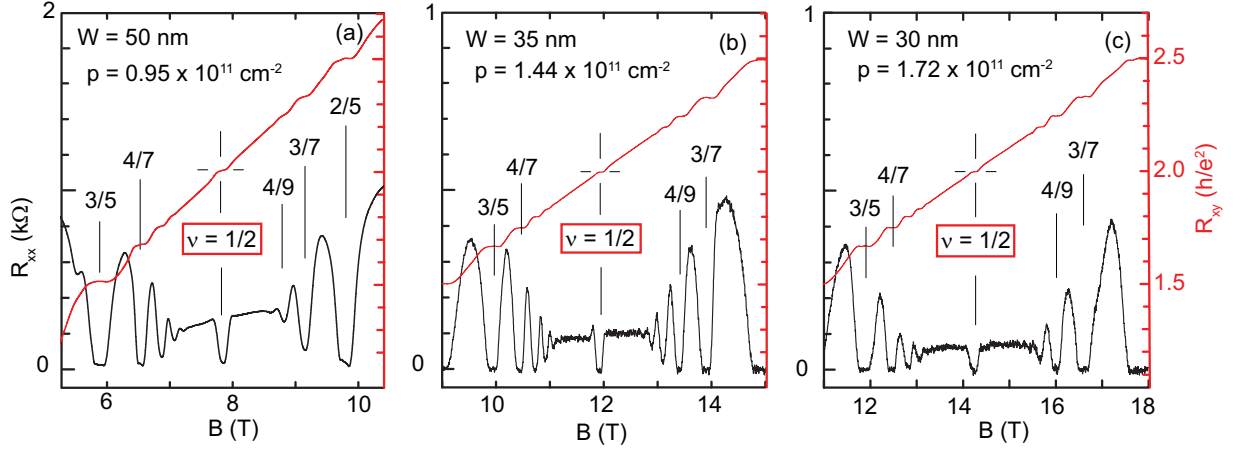


FIG. 1. (color online) Longitudinal (R_{xx}) and Hall (R_{xy}) resistance vs perpendicular magnetic field (B) traces taken at $T \simeq 30$ mK for the 50-, 35- and 30-nm-wide QWs at densities $p = 0.95, 1.44$ and $1.72 \times 10^{11} \text{ cm}^{-2}$, respectively.

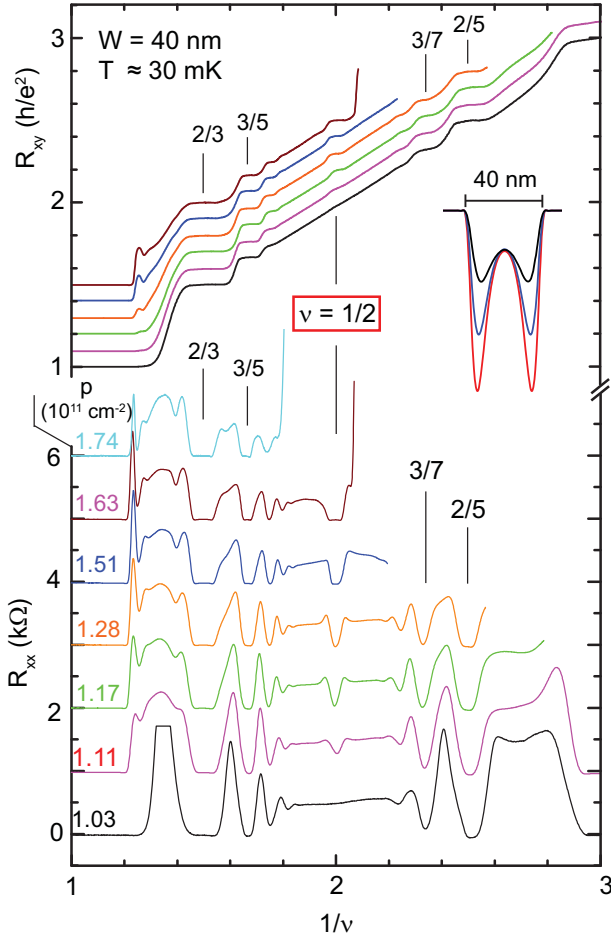


FIG. 2. (color online) Waterfall plots of R_{xx} and R_{xy} vs $1/\nu$ for the 40-nm-wide QW as p is changed from 1.03 to 1.74, while keeping the total hole charge distribution symmetric. Traces are shifted vertically for clarity. The $\nu = 1/2$ FQHE is not seen at the lowest p , and is replaced by an insulating phase at the highest p . The inset shows the calculated charge distribution for $p = 1.0$ (black), 1.5 (blue), and 2.0 (red).

$1/3, 2/5, 3/7, \dots$, and $2/3, 3/5, 4/7, \dots$, similar to what is seen in high-quality, single-subband, 2D electron or hole systems confined to narrow QWs. When we slightly increase p to $\simeq 1.11$, a FQHE emerges at $\nu = 1/2$, indicated by a dip in R_{xx} and a developing R_{xy} plateau. The R_{xx} minimum gets deeper and the R_{xy} plateau becomes flatter and wider as we continue to raise the density, indicating an increasingly stronger $\nu = 1/2$ FQHE. At $p = 1.51$, an insulating phase (IP) starts to emerge at low fillings (high fields) and moves towards higher fillings with increasing density. The IP reaches just to the low-filling side of the $\nu = 1/2$ FQHE at $p = 1.63$, and then at slightly higher density it destroys the $\nu = 1/2$ FQHE as it keeps moving to higher fillings.

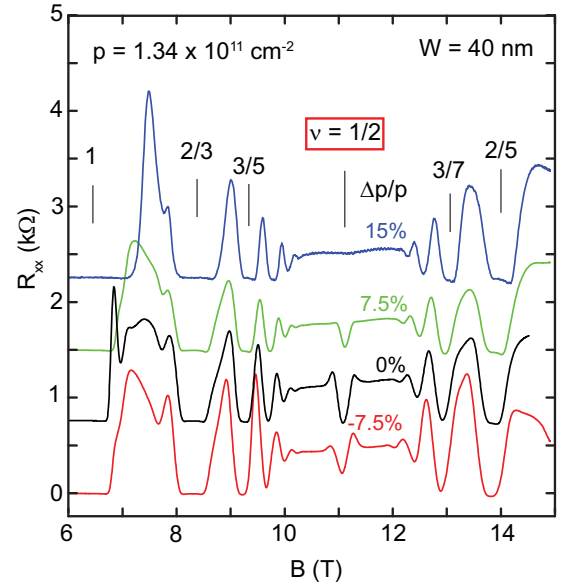


FIG. 3. (color online) R_{xx} vs B for the 40-nm-wide QW at a fixed density but different QW symmetries induced via applying front- and back-gate voltage biases.

The evolution seen in Fig. 2 is qualitatively very similar to the one seen in 2DESs confined to wide GaAs QWs [12, 21], with two notable exceptions in the FQHE to IP transition at high densities. First, in 2DESs, at the highest densities, when the system becomes very much bilayer-like, the IP moves to fillings near $\nu = 2/5$ [21], namely $1/5$ in each layer. This was attributed to the formation of a pinned Wigner crystal (WC); note that $1/5$ is indeed the filling near which a pinned electron WC is observed in high-quality, single-layer 2DESs [22–24]. In the 2DHS, on the other hand, at high densities, the IP moves to fillings larger than $2/5$. In another 40-nm-wide QW sample in which we can reach higher densities, the IP eventually approaches the $\nu = 2/3$ FQHE at $p \simeq 2.1$ when the system becomes quite bilayer-like. This is not unexpected. Low-density, single-layer 2DHSs are in fact known to exhibit an IP near $\nu = 1/3$, interpreted as a pinned hole WC [24–26]. The larger in-plane effective mass in GaAs 2DHSs, which causes significant LL mixing and renders the 2DHS effectively more dilute, is believed to be responsible for the higher ν near which the hole WC forms [24, 25]. Second, in 2DESs, for some particular density the IP is seen on both sides of a strong $\nu = 1/2$ FQHE [21]. In the 2DHS, however, we do not see such a reentrant IP. At $p = 1.63$ the IP is observed only on the low-filling side of the $\nu = 1/2$ FQHE. As p is slightly increased above 1.63, the $\nu = 1/2$ FQHE is quickly destroyed and the IP takes over at and near $\nu = 1/2$ (see the $p = 1.74$ trace in Fig. 2).

Returning to the $\nu = 1/2$ FQHE, in Fig. 3 we study this state in the 40-nm-wide QW at fixed $p = 1.34$ with different QW charge distribution symmetries. We change the symmetry by increasing the density by Δp via applying front-gate bias and decreasing the density by Δp via back-gate bias. The $\nu = 1/2$ FQHE is strong when the QW is symmetric ($\Delta p/p = 0$). It becomes weak when $\Delta p/p = \pm 7.5\%$ and is completely destroyed when $\Delta p/p = 15\%$. This evolution is also very similar to what is observed in 2DESs confined to wide GaAs QWs. For example, in a 77-nm-wide QW, the $\nu = 1/2$ FQHE is strong at density $n = 1.15$ when the QW is symmetric, and disappears when $\Delta n/n \gtrsim 7\%$ [12].

The data presented so far indicate that the $\nu = 1/2$ FQHE in 2DHSs exhibits qualitatively the same features as in 2DESs: It is only stable in symmetric QWs and at intermediate densities. For a closer, more quantitative comparison, in Fig. 4(a) we show a W vs density phase diagram for the ground state at $\nu = 1/2$ in 2DESs confined to wide GaAs QWs [17]. The yellow band is the region where the FQHE is the ground state of the 2DES. The 2DES becomes compressible in the lower left (green) region, and exhibits an IP in the upper right (red) region. In Fig. 4(a) we also show the 2DHS data by red symbols, but after shifting the y -axis (W) upward by 34 nm. The solid symbols represent the parameters for which we observe a $\nu = 1/2$ FQHE, and the open symbols rep-

resent the compressible phase (at low densities) or the IP (at high densities) in our 2DHSs. It is clear that, if we include the 2DHS data in Fig. 4(a) diagram without any adjustments in the QW width, all the data points would fall well below the yellow band and deep in the compressible region. Nevertheless, we will argue that the hole $\nu = 1/2$ FQHE in our 2DHSs has the same origin and is likely a two-component Ψ_{331} state.

First, the extreme sensitivity of the $\nu = 1/2$ FQH state to the 2DHS charge distribution symmetry (Fig. 3) provides clear evidence that its stability requires a delicate balance between the inter-layer and intra-layer interactions. Similar to the 2DES case [12], this observation strongly favors a two-component state.

Second, despite the apparent differences between the parameters of the 2DESs and 2DHSs in Fig. 4(a), it turns out that both systems in fact have very similar charge distributions when the $\nu = 1/2$ FQHE is stable. In Fig. 4(a) note that the density range where we observe the FQHE in the $W = 40$ nm hole QW is similar to the range where the FQHE is seen in 2DESs but with $W = 74$ nm, almost twice wider. In Figs. 4(b) and (c) we show the calculated charge distributions for electrons and holes, in 74- and 40-nm-wide QWs, respectively, both at a density of 1.50 when the $\nu = 1/2$ FQHE is strong. The calculations were done (at $B = 0$) by solving the Schrodinger and Poisson equations self-consistently; for the 2DHS, we used the 8×8 extended Kane model [27]. Despite the narrower well-width, thanks to the much heavier hole effective mass, the charge distribution of the holes is indeed bilayer-like and qualitatively very similar to the electrons'.

Now the Ψ_{331} state is theoretically expected to be stable when the intra-layer and inter-layer Coulomb energies, $e^2/4\pi\epsilon l_B$ and $e^2/4\pi\epsilon d$, respectively, are comparable [9, 11] ($l_B = \sqrt{\hbar/eB}$ is the magnetic length, d is the inter-layer distance, and ϵ is the dielectric constant). For an ideal bilayer carrier system (with zero layer thickness), the ratio d/l_B accurately reflects the relative strengths of the intra-layer and inter-layer Coulomb interactions and the Ψ_{331} FQHE at $\nu = 1/2$ should be observable for $d/l_B \lesssim 2$. However, in a system whose layer thickness, which we quantify as its full-width-at-half-maximum (λ in Figs. 4(b) and (c)), is comparable to or larger than l_B , the short-range component of the Coulomb interaction, which is responsible for the FQHE, softens [28, 29]. Associating the $\nu = 1/2$ FQHE with the Ψ_{331} state, it is thus not surprising that we see the FQHE in 2DHSs at a smaller $d/l_B \simeq 3.6$ compared to 2DESs ($d/l_B \simeq 6$) [17]: The short-range component of the intra-layer interaction is stronger for the 2DHS ($\lambda/l_B \simeq 1.4$) compared to the 2DES ($\lambda/l_B \simeq 2.7$); therefore to ensure the proper intra-layer to inter-layer interaction ratio which favors the Ψ_{331} state, a relatively stronger inter-layer interaction (larger $e^2/4\pi\epsilon d$) is also needed, implying a smaller d/l_B [12, 17]. In a sense, thanks to its smaller layer thickness, the 2DHS

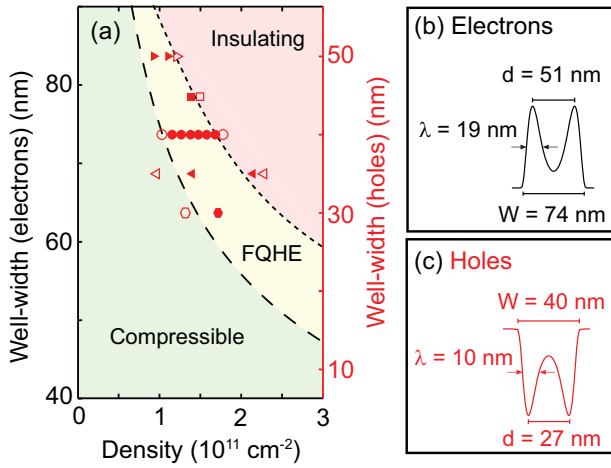


FIG. 4. (color online) (a) The well-width vs density phase diagram for different ground states observed at $\nu = 1/2$ in 2D *electron* systems confined to wide GaAs QWs (left axis) [17]. The yellow, red and green regions are where FQHE, insulating and compressible phases are observed, respectively. The red symbols (right axis, which is shifted upward by 34 nm relative to the left axis) are data points of 2DHSs. The solid symbols mark the parameters at which we observe the $\nu = 1/2$ FQHE in 2DHSs, and the open symbols are when the 2DHSs become compressible at low p or insulating at high p . The right panels show the charge distributions calculated for: (b) electrons at density 1.5 confined to a 74-nm-wide GaAs QW, and (c) holes at the same density to a 40-nm-wide GaAs QW. Despite the very different well-widths, the charge distributions are very similar for holes and electrons. In (b) and (c), we also mark the values of the inter-layer distance d and the “layer thickness” λ .

in a wide GaAs QW is closer to an ideal bilayer system.

Revisiting the phase diagram in Fig. 4(a), the empirical shift of the 2DHS data points by 34 nm clearly leads to a close matching of the regions where different phases (FQHE, compressible, and IP) are observed in the 2DESs and 2DHSs [30]. Absent of course is a rigorous theoretical justification for this shift which results in such a remarkable match.

Finally, we address another relevant energy scale, namely the pseudo-spin energy splitting. In 2DESs, the pseudo-spins are the symmetric (S) and anti-symmetric (A) electric subbands. Their energy separation, which is essentially the “inter-layer tunneling” energy, remains fixed as a function of B in the absence of interaction. In 2DHSs the situation is more complex because of the coexistence and mixing of HH and LH states. We illustrate this in Fig. 5 where we show the energy vs B LL diagram, calculated for a 2DHS confined to a symmetric 40-nm-wide QW at density $p = 1.5$ [27]. In our wide QWs with a sufficiently large density, the lowest two subbands are both HH-like near the subband edge. Yet B mixes the LH states into the wavefunction such that, at high field near $\nu = 1/2$, the three lowest-energy LLs (marked in red in Fig. 5) have $N = 0$ character. The

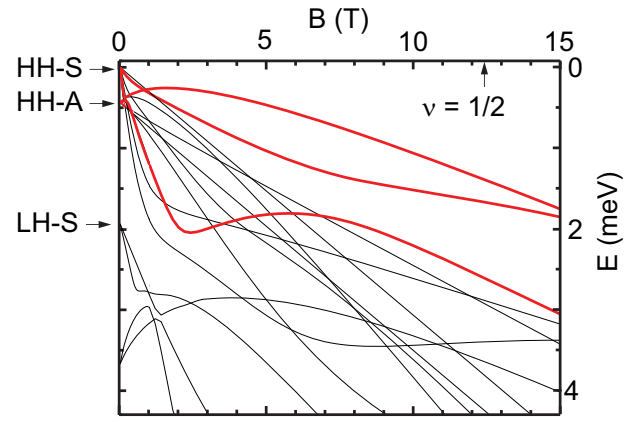


FIG. 5. (color online) Landau level fan diagram calculated for a 2DHS confined to a 40-nm-wide QW at $p = 1.5$. The three lowest-energy levels, which have $N = 0$ character at high fields near $\nu = 1/2$ ($B = 12.3$ T), are shown in red.

pseudo-spin energy splitting is therefore of the order of the separation between these energy levels at $B = 12.3$ T which is smaller than $\simeq 10$ K, or $\simeq 0.06$ in units of $e^2/4\pi\epsilon l_B$. This is comparable to the values for 2DESs when $\nu = 1/2$ FQHE is seen at similar densities [12, 17], and is consistent with the Ψ_{331} state when the intra-layer Coulomb energy dominates over the pseudo-spin energy separation.

We acknowledge support from the DOE BES (DE-FG02-00-ER45841) for measurements, and the Gordon and Betty Moore Foundation (GBMF2719), the Keck Foundation, and the NSF (DMR-1305691 and MRSEC DMR-0819860) for sample fabrication. Work at Argonne was supported by DOE BES under Contract No. DE-AC02-06CH11357. A portion of this work was performed at the National High Magnetic Field Laboratory, which is supported by NSF Cooperative Agreement No. DMR-1157490, by the State of Florida, and by the DOE. We thank J. K. Jain and Z. Papić for illuminating discussions, and S. Hannahs, E. Palm, J. H. Park, T. P. Murphy, and G. E. Jones for technical assistance.

-
- [1] D. C. Tsui, H. L. Stormer, and A. C. Gossard, *Phys. Rev. Lett.* **48**, 1559 (1982).
 - [2] J. K. Jain, *Composite Fermions* (Cambridge University Press, Cambridge, UK, 2007).
 - [3] R. L. Willett, J. P. Eisenstein, H. L. Störmer, D. C. Tsui, A. C. Gossard, and J. H. English, *Phys. Rev. Lett.* **59**, 1776 (1987).
 - [4] Y. W. Suen, L. W. Engel, M. B. Santos, M. Shayegan, and D. C. Tsui, *Phys. Rev. Lett.* **68**, 1379 (1992).
 - [5] J. P. Eisenstein, G. S. Boebinger, L. N. Pfeiffer, K. W. West, and S. He, *Phys. Rev. Lett.* **68**, 1383 (1992).
 - [6] G. Moore and N. Read, *Nuclear Physics B* **360**, 362 (1991).

- [7] C. Nayak, S. H. Simon, A. Stern, M. Freedman, and S. Das Sarma, *Rev. Mod. Phys.* **80**, 1083 (2008).
- [8] B. I. Halperin, *Helv. Phys. Acta* **56**, 75 (1983).
- [9] D. Yoshioka, A. H. MacDonald, and S. M. Girvin, *Phys. Rev. B* **39**, 1932 (1989).
- [10] Y. W. Suen, M. B. Santos, and M. Shayegan, *Phys. Rev. Lett.* **69**, 3551 (1992).
- [11] S. He, S. Das Sarma, and X. C. Xie, *Phys. Rev. B* **47**, 4394 (1993).
- [12] Y. W. Suen, H. C. Manoharan, X. Ying, M. B. Santos, and M. Shayegan, *Phys. Rev. Lett.* **72**, 3405 (1994).
- [13] Z. Papić, G. Möller, M. V. Milovanović, N. Regnault, and M. O. Goerbig, *Phys. Rev. B* **79**, 245325 (2009).
- [14] Z. Papić, N. Regnault, and S. Das Sarma, *Phys. Rev. B* **80**, 201303 (2009).
- [15] M. R. Peterson and S. Das Sarma, *Phys. Rev. B* **81**, 165304 (2010).
- [16] M. R. Peterson, Z. Papić, and S. Das Sarma, *Phys. Rev. B* **82**, 235312 (2010).
- [17] J. Shabani, Y. Liu, M. Shayegan, L. N. Pfeiffer, K. W. West, and K. W. Baldwin, *Phys. Rev. B* **88**, 245413 (2013).
- [18] M. Greiter, X.-G. Wen, and F. Wilczek, *Phys. Rev. Lett.* **66**, 3205 (1991).
- [19] D.-K. Ki, V. I. Fal'ko, and A. F. Morpurgo, *arXiv:1305.4761* (2013).
- [20] As discussed elsewhere [Yang Liu *et al.*, unpublished], for 2D holes confined to the 30- and 35-nm-wide QWs, at low densities we also observe a $\nu = 1/2$ at an unusual crossing of the hole LLs. The data presented here were taken far from such LL crossings.
- [21] H. C. Manoharan, Y. W. Suen, M. B. Santos, and M. Shayegan, *Phys. Rev. Lett.* **77**, 1813 (1996).
- [22] H. W. Jiang, R. L. Willett, H. L. Stormer, D. C. Tsui, L. N. Pfeiffer, and K. W. West, *Phys. Rev. Lett.* **65**, 633 (1990).
- [23] V. J. Goldman, M. Santos, M. Shayegan, and J. E. Cunningham, *Phys. Rev. Lett.* **65**, 2189 (1990).
- [24] M. Shayegan, in *Perspectives in Quantum Hall Effects*, edited by S. D. Sarma and A. Pinczuk (Wiley, New York, 1998) pp. 343–383.
- [25] M. B. Santos, Y. W. Suen, M. Shayegan, Y. P. Li, L. W. Engel, and D. C. Tsui, *Phys. Rev. Lett.* **68**, 1188 (1992).
- [26] C.-C. Li, L. W. Engel, D. Shahar, D. C. Tsui, and M. Shayegan, *Phys. Rev. Lett.* **79**, 1353 (1997).
- [27] R. Winkler, *Spin-Orbit Coupling Effects in Two-Dimensional Electron and Hole Systems* (Springer Berlin Heidelberg, Berlin, 2003).
- [28] M. Shayegan, J. Jo, Y. W. Suen, M. Santos, and V. J. Goldman, *Phys. Rev. Lett.* **65**, 2916 (1990).
- [29] S. He, F. C. Zhang, X. C. Xie, and S. Das Sarma, *Phys. Rev. B* **42**, 11376 (1990).
- [30] A scaling of the 2DHS QW well-width by a factor of $\simeq 74/40$ also leads to a reasonable agreement between the 2DHS and 2DES data, but the agreement is not as good as the one we find by the shifting.